

The Layered Transition Metal Dichalcogenides as Materials for Storage Clean Energy: Ab initio Investigations

S. Meziane, H. I. Faraoun, C. Esling

Abstract—Transition metal dichalcogenides have potential applications in power generation devices that convert waste heat into electric current by the so-called Seebeck and Hall effects thus providing an alternative energy technology to reduce the dependence on traditional fossil fuels. In this study, the thermoelectric properties of 1T and 2HTaX₂ (X= S or Se) dichalcogenide superconductors have been computed using the semi-classical Boltzmann theory. Technologically, the task is to fabricate suitable materials with high efficiency. It is found that 2HTaS₂ possesses the largest value of figure of merit ZT= 1.27 at 175 K. From a scientific point of view, we aim to model the underlying materials properties and in particular the transport phenomena as mediated by electrons and lattice vibrations responsible for superconductivity, Charge Density Waves (CDW) and metal/insulator transitions as function of temperature. The goal of the present work is to develop an understanding of the superconductivity of these selected materials using the transport properties at the fundamental level.

Keywords—Ab initio, high efficiency, power generation devices, transition metal dichalcogenides.

I. INTRODUCTION

LAYERED transition metal dichalcogenides MX₂ (M= transition metal, X= S, Se, or Te) are of particular importance for their rich variety of the physical properties. These two-dimensional (2D) compounds are relatively simple and Pauli paramagnet systems which exhibit a range of CDW transitions [1], [2], superconducting behavior at low temperatures [3], optical band gaps [4], [5], usefulness for solar cells [6], [7], and potential as catalysts for hydrogen evolution [8] and CO₂ reformation [9]. Then, they have been widely used in electrochemical applications, metallurgical process control, coal gasification, and environmental pollution control [10].

The properties of CDW in a transition metal dichalcogenide TaX₂ have been the subject of intensive studies [1]. Around room temperature, the compounds show the nearly commensurate (NC) CDWs with hexagonal domains separated by domain walls, where the CDW phases abruptly change. With decreasing temperature, the domain size becomes large, and the NC CDWs are transformed into the commensurate (C)

S. Meziane is with Ecole Supérieure des Sciences Appliquées – ESSAT-Tlemcen, Algeria (phone: +213(0)43415541; e-mail: s.meziane@epst-tlemcen.dz).

H. I. Faraoun was with Tlemcen University, Algeria (e-mail: houda_imane@ymail.com).

C. Esling was with Lorraine University, Metz, France (e-mail: claude.esling@univ-lorraine.fr).

CDW states with a resistivity jump at low temperatures [11]. On the other hand, almost 30 years ago, of high temperature superconductors having T_c's exceeding 100 K. Most recently, a range of Fe-pnictide and chalcogenide compounds have been shown, unexpectedly, to exhibit SC in the 50 K range [12]. This fact, a coexistence of superconductivity and CDW states are predicted in these material classes. The diversity of the behaviors from family to family might indicate that both orbital and spin scenarios are necessary to fully understand the iron based superconductors [13].

The energy storage procedures are reviewed, together with a discussion of electricity generating methods and future electricity use [14]. The areas such as improved engine-management of internal combustion engine vehicles and improved batteries for electric vehicles, where progress depends very much on materials developments, are surveyed in more detail. The need for developing a cheap, yet effective method of converting solar energy into electrical or chemical energy stimulated rapid advancement of semiconductor electrochemistry in the past decades. For designing and using such materials, the crystallographic data, electronic and thermoelectric transport properties are of considerable significance. Depending on the temperature, pressure, and the chalcogen atoms, many polymorphic modifications as 1T (octahedral coordination) and 2H (trigonal prismatic coordination) polytypes are shown. Experimentally, growth of these compounds was made via the chemical vapor transport (CVT) by the usual iodine method [15]. At ambient conditions, hexagonal 2H type is the stable structure for TaX₂. These compounds are of great interest because the behavior of resistivity, particularly of 1T TaS₂ (Se₂) has been termed anomalous because the proposed band structure of 1T-materials by Wilson and Yoffe predicts a partially filled high density of states (DOS) d-band metal [16]. Many literatures, including some review articles are available. However, data hamper uses in establishing a robust data base of the theoretical study of thermoelectric transport properties of TaX₂ dichalcogenides are barely debated.

In this report, superconductivity, CDW and metal/insulator transitions for 1T and 2H TaX₂ phases in dependence of the temperature, have been investigated. Heat capacity, Hall effect, Pauli magnetic susceptibility, electrical and thermal conductivities, Seebeck effect and figure of merit are computed, by means of the semi-classical Boltzmann theory. The relationships between superconductivity, CDW on metal – insulator transitions and thermoelectric transport properties

have been discussed, in order to understand the physical anisotropy of TaX₂ compounds. Indeed, at low temperatures, the atoms move out of their equilibrium positions generating a significant periodic lattice distortion, which causes transition phases and the appearance of the CDW states. For the simplest case of 1T TaSe₂, the room temperature superlattice is realized when the existing CDW rotates into an orientation from which it then becomes commensurate. Wilson et al found that this condition produces a gap in the electron DOS at the Fermi level [1]. For 2H polytypes though CDW formation is withheld to low temperatures, probably because of the more complex band structure [16]. Thus, many efforts have been devoted to combine crystallographic and electronic structure properties for the purpose of optimizing the thermoelectric performances. For instance, electronic DOS at the Fermi level is required to maximize the ZT (figure of merit), which was recently demonstrated experimentally in terms of band engineering. at the Fermi level is required to maximize the ZT (figure of merit), which was recently demonstrated experimentally in terms of band engineering. The main motivation of this review is to extend the previous experimental and theoretical study, by addressing the electronic structure and thermoelectric properties of TaX₂ compounds.

II. METHODOLOGY

In order to obtain more insight into the effect of the superconductivity and phase transformations to the electrical and thermal conductivities in the TaX₂ dichalcogenides which tantalum ions are coordinated in trigonal prisms of sulfur ions [17] or octahedral sites, the transport properties are computed. Several models have been proposed to explain the interlayer magneto-transport in high-T_c superconductors [18].

Thermoelectric properties such as Hall coefficient, Seebeck tensor, electrical and thermal conductivities are derived by making use of Boltzmann's transport theory incorporating the constant relaxation time approximation. The interactions have the consequence that the conduction carriers are not in their equilibrium states. There are two approaches to such a non-equilibrium transport, namely the Green – Kubo theory [19] and the semi – classical Boltzmann transport theory [20], [21]. The former relates transport coefficients to the correlation function of the current or heat flux. The later treats effect of various scattering mechanisms on transport properties in terms of relaxation times. The Boltzmann transport theory has proven its validity in numerous applications where calculated transport coefficients can be readily compared with experimental results. Accordingly, it is shown how to merge the electronic structure – as derived from a first-principles approach – into the Boltzmann theory for deriving the electronic transport coefficients. In this study, the Boltzmann theory that has been used describes the electron system by introducing a distribution function, which is given by the Fermi function when electrons are in the equilibrium state. A program package called BoltzTrap [18] is adopted to incorporate the necessary output from the Wien2k calculations. It is based on a smoothed Fourier interpolation of

the band energies where the space group symmetry is maintained by using star functions [22]. From this analytical representation, the necessary derivatives are calculated for the transport distributions. The electrical conductivity is calculated using the relation [23], [24].

III. RESULTS AND DISCUSSIONS

A. Specific Heat

The temperature dependence of the heat capacity (specific heat) of TaX₂ from 0 to 700 K is presented in Fig. 1, which shows a discontinuity at the anomaly temperature, suggesting that the compounds have a first order phase transition in the temperature range 70-180 K. From these data, we were able to get that the strong interaction between the electrons and phonons have been responsible for the formation of the commensurate charge density wave (CCDW) phases. This result is in agreement with the specific heat value observed by [25] for 2H-TaS₂ using an AC calorimeter method.

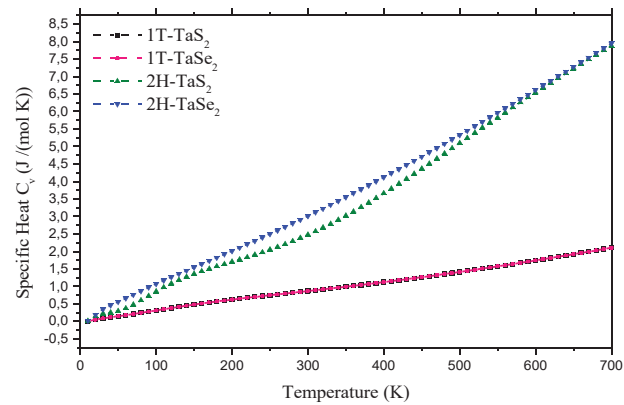


Fig. 1 Evolution of specific heat versus temperature of TaX₂

B. Hall Coefficient

Fig. 2 shows the temperature dependence of the Hall coefficient (RH) of TaX₂. The values of RH were positive for 1T TaX₂, negative for 2H TaSe₂, and scarcely dependent on temperature for these samples, indicating a typical metallic nature with hole and electron conduction, respectively. These values were negligible and almost independent of temperature for all compounds, except for 2H TaS₂. In this last system two regions are detected: at low temperatures, 2H TaS₂ shows an anomalous sign change in the Hall coefficient, probably associated with a magnetic ordering at about ~ 90 K, then becomes stable starting from 300 K. Indeed, a small degree of magnetic ordering is also present in this compound in the low temperature region. This is illustrated in Fig. 3 which represents the temperature dependence of Pauli magnetic susceptibility of TaX₂ dichalcogenides, at which the Hall coefficient begins the rapid change from p- to n-type conducting. Second region begins above 300 K with small positive and constant value of RH independently of the temperature. Hall coefficient can also be calculated from the electrical conductivity. The decreasing tendency of RH with decreasing temperature below 300 K for 2H TaS₂ indicates

that this compound is semiconductor rather than metal, and then anomalous behavior at the transition temperature has been observed, presumably due to the apparition of the CDW phase. The large change in the Hall coefficient near the CDW transition is similar to that observed for third-row transition metal dichalcogenides NbS₂ and VSe₂ at the CDW transition. Experimentally, similar results were found by A.H. Thompson et al. of 2H TaS₂ with RH = +2.2 × 10⁻¹⁰ m³ C⁻¹ at 300 K [26].

C. Pauli Magnetic Susceptibility and Superconductivity

The Pauli magnetic susceptibility is proportional to the DOS at the Fermi surface in any electron gas. The temperature dependence of magnetic susceptibility is displayed in Fig. 3. The susceptibility increases with decreasing temperatures, following the Curie-Weiss law. For all compounds, the results show that the susceptibility is relatively temperature independent at higher temperatures. It can be seen in the figure that the superconductivity transition temperature is about K with different intensities for all compounds.

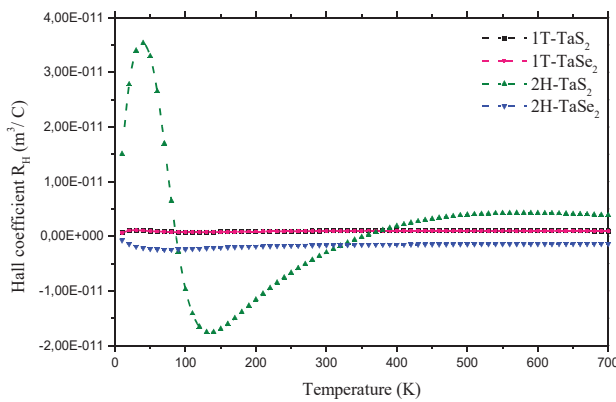


Fig. 2 Evolution of Hall coefficient versus temperature of TaX₂

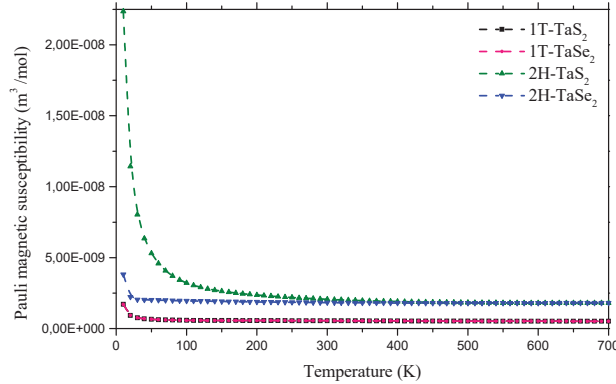


Fig. 3 Evolution of Pauli magnetic susceptibility versus temperature of TaX₂

D. Hall Mobility

Fig. 4 shows the temperature variations of the Hall mobility. The rather small values of μ_H suggest that there are many scattering factors in the samples, i.e. impurities, vacancies, dislocations, grain boundaries, etc. A singular behavior has been noticed for 2H TaS₂ with the mixed conduction of

electrons and holes as compared to the rest of the samples. The presence of donor levels may be a possible origin of this conductivity, hardly assuming the existence of a large amount of vacancies. Indeed, the energy band calculations clarify these issues. The somewhat large concentration of holes observed in 2H TaS₂ may indicate that a small number of Ta vacancies remain even in the stoichiometric sample. At high temperature, high-mobility and low-density holes compensate the contribution of electrons to the Hall conductivity.

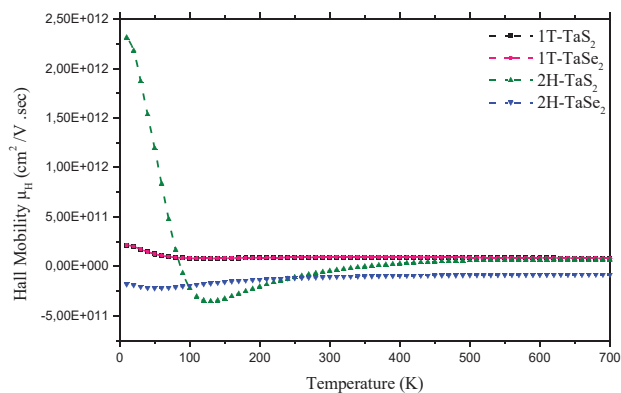


Fig. 4 Evolution of Hall mobility versus temperature of TaX₂

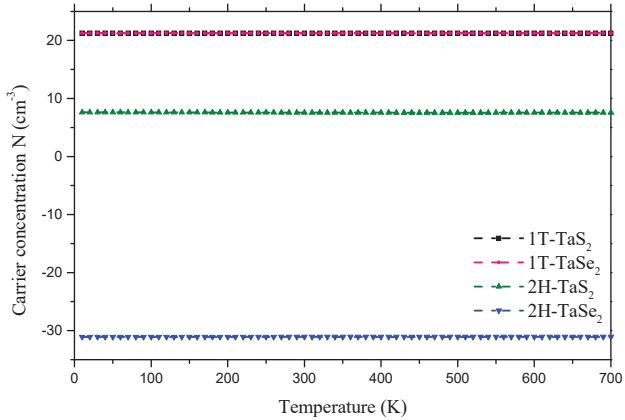


Fig. 5 Evolution of carrier concentration versus temperature of TaX₂

From the Weidmann-Franz law, it is evident that throughout the studied temperature range, heat transport is essentially due to the lattice contribution. At the lower temperatures the absence of any T⁻¹ Law behavior has been observed, generally ascribed either to electron – phonon interaction or to scattering by static dislocations. However, for layer structures, one also has to take into account the anisotropy of the phonon branches. Such an approach was carried out for graphite by [27].

E. Carrier Concentrations

The carrier concentrations (n) shown in Fig. 5 are calculated assuming one carrier type, from room temperature Hall constants. The values of charge concentrations are found to be 21.34, 7.56 and -31.20 cm⁻³ for 1T TaX₂, 2H TaS₂ and 2H

TaSe₂ respectively, indicating that the transport in 1T TaX₂ has been carried by the holes because the positive values, and the transport in 2H TaS₂ has been carried by electrons because the negative value of charge concentration. These numbers show small or no variations with temperature in the whole range 0-700 K, suggesting that the samples are metals.

F. Seebeck Coefficient

To investigate the conduction mechanism in more detail, Seebeck coefficients have been determined from 0 to 700 K for all samples in Fig. 6. A broad peak has been observed in the temperature range 70-180 K. Three transition regions are observed: coexistence of superconductivity and CDW phases at low temperatures from 0.7 to 10 K. Further, an incommensurate and then commensurate CDW phase are shown at 180 K and 70 K, respectively. Finally, linear temperature dependence above the CDW transition from 300 to 700 K for the normal phases is noticed. Around the lower temperatures, strong influences of the CDW phase transitions on the electronic states exist. Since the CDW consists of the coupled modulations of the conduction electron density and atomic positions, it produces an energy gap at the Fermi surface, because of phonon effects. The anomalies are sharper compared to those observed in the electrical resistivity and the Pauli magnetic susceptibility.

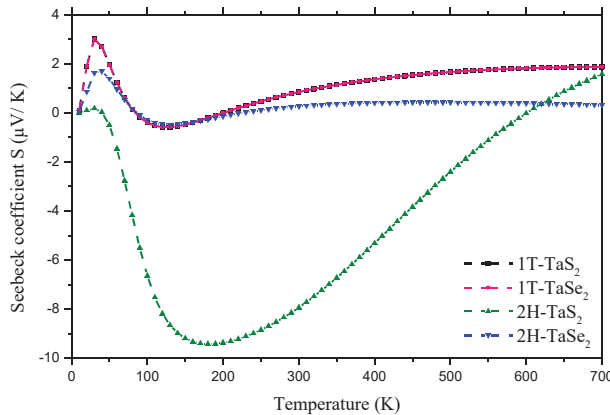


Fig. 6 Evolution of Seebeck coefficient versus temperature of TaX₂

Also, CDW of the compounds is more sensitive to the change in the DOS at the Fermi surface, it has been noticed a sharp feature at the transition, where the carrier density changes, illustrated by the Hall coefficient curves. These discontinuities are due to the strong interaction between the free carriers and phonons. The positive Seebeck coefficient reveals the dominance of the holes such as the charge carrier conduction, whereas the negative sign of the thermoelectric power is adequate of the electrons as charge carriers dominant. At high temperature, all compounds show positive values of Seebeck coefficient occurred if the electrons of higher energy in the d band of tantalum are more scattered, compared to the low-energy electrons. The larger value of Seebeck coefficient is discerned of 2H TaS₂ equal to $-94 \mu\text{V/K}$ at 180 K, reaches maximum then declines continuously above 300 K, in good

agreement with the value of Seebeck coefficient found in experimental results for PbSe₂ equal to $+99 \mu\text{V/K}$ at 400 K studied by [28]. Results presented in this study are in good concordance with those of [29], [30] using the Born von Karman model and those presented by A.H. Thompson et al. of 2H TaS₂, with $S = -7 \mu\text{V/K}$ at 300 K [26].

G. Electrical Resistivity

Fig. 7 shows the temperature dependence of the electrical resistivity in the range 0 to 700 K. The resistivity gradually decreases with decreasing temperature, exhibiting superconductivity behavior and CDW transitions at low temperatures. This indicates that at temperatures just above the superconducting T_c , most likely dominated by grain boundary or impurity scattering [31] who can facilitate the lattice distortion (CDW transition), like the effect of pressure shown by [32], where it has been noticed that in the presence of hydrostatic pressure, the CDW transitions shift to high temperature. The strains and the impurities inside the crystals give rise to the increased overlap of the tantalum's narrow d band with the s-p bands of sulfur (or selenium), in turn increasing the CDW onset temperature, observed for 2H TaS₂ in good agreement with the experimental results obtained by [26].

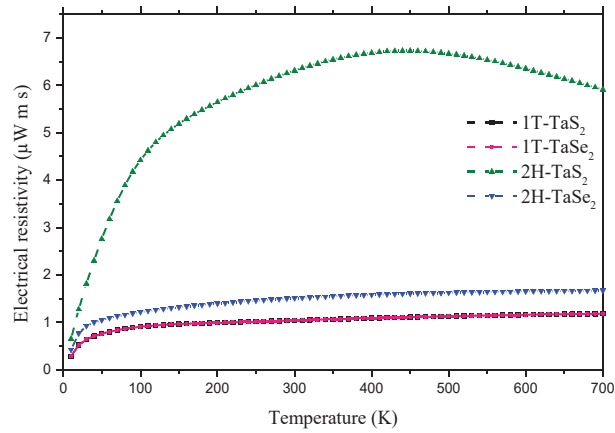


Fig. 7 Evolution of electrical resistivity versus temperature of TaX₂

The value of $\rho = 1.5 \times 10^{-6} \Omega\text{m}$ at 300 K [26] has been found, a change of slope at 75 K and 82 K for CDW transitions have been measured by [33] and [34] of 2H TaS₂ and 2H TaSe₂ respectively, in good agreement with our calculations. Also, a superconducting transition at 0.8 K has been found by [35] of 2H TaS₂. Secondly, the more electronegative sulfur renders the structure of TaS₂ more ionic than that of TaSe₂, so that a larger electrical resistivity is expected for the 2H TaS₂, and a large value of Seebeck coefficient. This anisotropy establishes that these compounds are quasi-two dimensional metals, as expected from crystal structures data and the electronic density d states [36]. This temperature dependence of resistivity for TaX₂ implies that the strains and the impurities (vacancies or dislocations) play a significant role of this behavior.

H. Electrical Conductivity

Curves of electrical conductivity have the same shape and become linear above CDW transitions (Fig. 8). Superconducting transitions have been observed at 3 K for 1T TaX₂, 2.2 K and 0.8 K for 2H TaS₂/Se₂, respectively. Fleming and Colman [37] have reported that the superconducting critical temperature of TaS₂ was enhanced to about 3.5 K for 2H Fe 0.05 TaS₂. This exponential decay of electrical conductivity has been probably due to the drastic alteration in the Fermi level. It can be seen that two regimes characterize the conductivity versus temperature: (1) 0 K < T < 100 K, abrupt and important decrease of the electrical conductivity of all compounds is observed, indicating the occurrence of conductor-semiconductor phase transition; (2) around T 100 K, conductivity decreases slightly when the temperature increases. Such a variation is characteristic of a metallic behavior. This result supports the experimental observation made by [35] and [38] that at the transition temperature, a metal-insulator/metal-semiconductor transition is occurring in TaX₂. Indeed, metal-metal bonding may arise from a direct overlap of metal orbitals. However, an indirect interaction between metal atoms is also possible. It is shown that the presence of a highly medium polarization around positively charged metal atoms leads to an effective metal-metal interaction. In insulating ionic compounds, the anions serve as the medium polarization. This leads to a clustering of metal atoms in layers or chains in compounds with highly polarizable anions. In compounds with metallic conduction, like TaX₂ the conduction electrons provide the medium polarization. The instability of conduction electrons in linear-chain and layered compounds leads to CDW and the associated clustering of metal atoms [39].

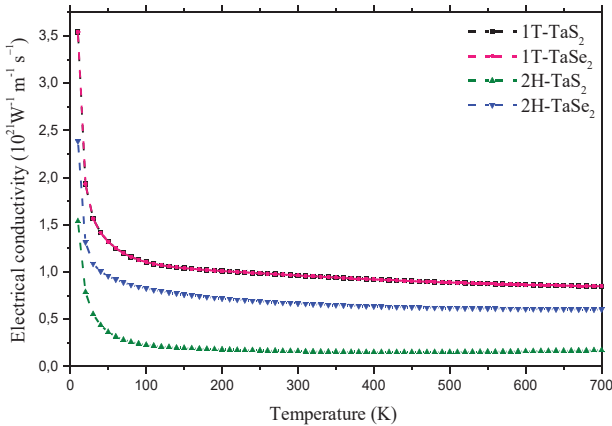


Fig. 8 Evolution of electrical conductivity versus temperature of TaX₂

I. Thermal Conductivity

The thermal conductivity versus temperature curves for all TaX₂ compounds are shown in Fig. 9. Large increase of thermal conductivity has been noticed at the transition temperatures, from the CDW to the normal phases. The gradually increase of the thermal conductivity with

temperature shows metallic behavior. This is mainly due to the increase in the number of phonon's which are seen to be most strongly affected by the transition. Then, at low temperature range the lattice contribution is more dominant than the electronic contribution while with increasing temperature the electronic contribution becomes predominant. The values of the thermal conductivities are comparable to those found in thermoelectric materials such as Bi₂Te₅ ($\kappa = 2.5 \text{ W m}^{-1} \text{ K}^{-1}$) [40], and with the experimental result of [41], and that observed by [42]. This trend is in good agreement with the results presented in this study.

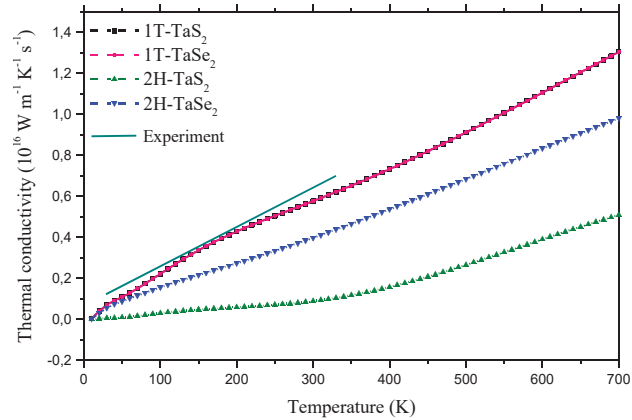


Fig. 9 Evolution of thermal conductivity versus temperature of TaX₂

J. Figure of Merit

In Fig. 10, the variation of the figure of merit ZT with temperature has also been plotted for TaX₂. The dimensionless figure of merit ZT of TaX₂ is evaluated by using the data of the electrical resistivity, Seebeck coefficient and thermal conductivity. It was observed that the ZT of 2H-TaS₂ is the largest value, equal to 1.27 at 175 K. Above 300 K, very low values of ZT are observed for all TaX₂, probably due to the low absolute values of Seebeck coefficients and electrical conductivities, in addition to the high value of electronic thermal conductivity.

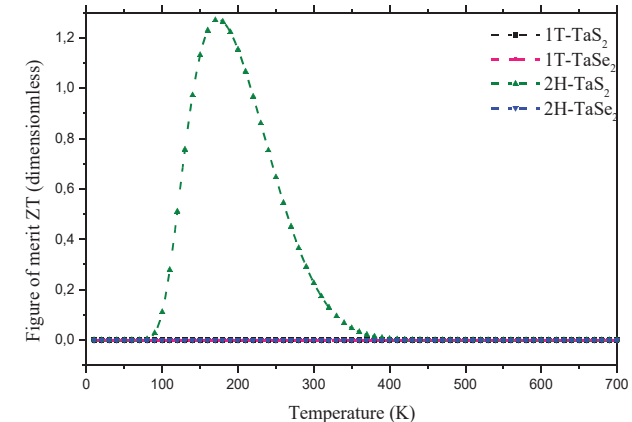


Fig. 10 Evolution of figure of merit versus temperature of TaX₂

In order to utilize the TaX_2 dichalcogenides in actual thermoelectric applications, it is necessary to optimize the electrical transport properties. In addition, further improvements of the figure of merit may be achieved by doping to optimize the number of charge carriers. When the charge carrier concentration increases, the Seebeck coefficient is expected to decrease whilst the electrical conductivity is expected to increase, and a maximum in the power factor will be found for a certain charge carrier concentration (10^{19} carriers cm^{-3} for broad band semiconductors) [40].

IV. CONCLUSION

The research of new materials with original properties for different applications is one of the intents in the activity of scientists. The study of thermoelectric properties of transition metal dichalcogenide superconductors is among these purposes. Thus, the transition metal dichalcogenides and their intercalates, while s-wave superconductors, contain many examples that are not at all conventional in their superconducting and normal state properties [43]. The aim of this review is to point out that there are many rich scientific phenomena and new technological opportunities underlying highly thermoelectric materials [44].

For TaX_2 dichalcogenides, understanding of anisotropic physical properties like CDW transitions, superconductivity, metal – insulator transitions and the metallic states are needed to optimize the thermoelectric transport properties for energy harvesting. In this case, we can establish that the electron-phonon coupling driven superconductivity at the onset of CDW states. Then, new and attractive candidates which may have large figure of merit ZT with high Seebeck coefficient, large electrical conductivity and low thermal conductivity to obtain high energy density and rate capability are needed. The challenge of the applications requires ZT higher than 1. Experimentally, it is known that the metal – insulator transition temperature of TaX_2 is very sensitive to the purity of chemicals used for crystal growth and the growth conditions, such as temperature and pressure [45]. Satisfying of all these criterions is impossible and the compromise between those is required. Preparation of the TaX_2 with different compositional deviations from stoichiometry is one of the ways of changing the carrier concentration optimized by appropriate doping, and hence affecting the value of power factor.

The present thermoelectric transport properties are successfully applied to comprehend the experimental findings for TaX_2 dichalcogenides. In particular, importance of the transport properties is the variation of stoichiometry of the samples, phase transformations depending on the temperature, and more theoretical comprehension of the crystallographic structures and electronic states of these compounds. The results in terms of numbers and analysis manifest the importance and capabilities of first – principles computational materials design.

REFERENCES

- [1] J.A. Wilson, F.J. Di Salvo and S. Machajan, Charge-density waves and superlattices in the metallic layered transition metal dichalcogenides, *Adv. Phys.* 24 (1975) 117-201.
- [2] V. Vescoli, L. Degiorgi, H. Berger and L. Forro, The optical properties of the correlated two-dimensional 2H-TaSe₂ system, *Synthetic Metals* 103 (1999) 2655-2657.
- [3] E. Morosan, H.W. Zandbergen, B.S. Dennis, J.W.G. Bos, Y. Onose, T. Klimeczuk, A.P. Ramirez, N.P. Ong, R.J. Cava, Superconductivity in Cu x TiSe₂, *Nat. Phys.* 2 (2006) 544-550.
- [4] C.M. Fang, R.A. de Groot, C. Haas, Bulk and surface electronic structure of 1T-TiS₂ and 1T-TiSe₂, *Phys. Rev. B* 56 (1997) 4455-4463.
- [5] A. Ramasubramanian, D. Naveh, E. Towe, Tunable band gaps in bilayer transition-metal dichalcogenides, *Phys. Rev. B* 84 (2011) 205325.
- [6] K.S. Chandra Babu, O.N. Srivastava, Photoelectrochemical solar cells based on TiS₂/TiO₂(TiOxSy) photoelectrodes, *Cryst. Res. Technol.* 23 (1988) 4.
- [7] H. Tributsch, Ber. Bunsenges., Layer-Type Transition Metal Dichalcogenides - A New Class of Electrodes for Electrochemical Solar Cells, *Phys. Chem.* 81 (1977) 361-369.
- [8] B. Hinemann, P.G. Moses, J. Bonde, K.P. Jorgensen, J.H. Nielsen, S. Horch, I. Chorkendorff, J.K. Norskov, MoS₂ nanoparticles for hydrogen evolution: A combined UHV/STM and electrochemical study, *J. Am. Chem. Soc.* 127 (2005) 5308-5309.
- [9] T. Osaki, T. Horiuchi, K. Suzuki, T. Mori, Catalyst performance of MoS₂ and WS₂ for the CO₂ -reforming of CH₄ Suppression of carbon deposition, *Appl. Catal. A* 155 (2) (1997) 229- 238.
- [10] J. Rouxel, Chalcogénures Lamellaires et Intercalaires Alcalins, Materials Science and Engineering 31 (1977) 277-280.
- [11] E. Endo, S. Nakao, W. Yamaguchi, T. Hasegawa, K. Kitazawa, Influence of CDW stacking disorder on metal-insulator transition in 1T-TaS₂, *Solid State Communications* 116 (2000) 47-50.
- [12] F. Kneidinger, E. Bauer, I. Zeiringen, P. Rogl, C. Blaas-Schenner, D. Reith, R. Podloucky, Superconductivity in non-centrosymmetric materials, *Physica C* 514 (2015) 388- 398.
- [13] C.C. Chang, T.K. Chen, W.C. Lee, P.H. Lin, M.J. Wang, Y.C. Wen, P.M. Wu, M.K. Wu, Superconductivity in Fe-chalcogenides, *Physica C* 514 (2015) 423-434.
- [14] B.C. Tofield, Materials for Energy Conservation and storage, *Applied Energy* 8 (1981) 89-142.
- [15] Koji Horiba, Kanta Ono, Han Woong Yeom, Yoshihiro Aiura, Osamu Shiino, Jin Ho Oh, Takayuki Kihara, Shinsuke Nakazono, Masaharu Oshima, Akito Kakizaki, Angle-resolved photoemission study in the commensurate CDW phase of 1T-TaSe₂, *Physica B* 284-288 (2000) 1665-1666.
- [16] Sangeeta Sharma, S. Auluck and M. A. Khan, Optical properties of 1T and 2H phase of TaS₂ and TaSe₂, *Pramana, I. Phys.* 54 (1999) 431-440.
- [17] Hiroya Sakurai, Yoshihiko Ihara, Kazunori Takada, Superconductivity of cobalt oxide hydrate, Na_x(H₃O)_zCoO_{2-y}H₂O, *Physica C* 514 (2015) 378-387.
- [18] P. Samuely, P. Szabo, J. Kacmarcik, A.G.M. Jansen, A. Lafond, A. Meerschaut, A. Briggs, Two dimensional behavior of the naturally layered superconductor (LaSe)_{1.14}(NbSe₂), *Physica C* 369 (2002) 61-67.
- [19] R. Kubo, Statistical-Mechanical Theory of Irreversible Processes. I. General Theory and Simple Applications to Magnetic and Conduction Problems, *Journal of the Physical Society of Japan*, 12 (1957) 570-586.
- [20] J.M. Ziman, Electrons and Phonons: The Theory of Transport Phenomena in Solids, Oxford University Press, USA, 2001, pp. 1-56.
- [21] R.H. Bube, W.H. McCarroll, Photoconductivity in indium sulfide powders and crystals, *J. Phys. Chem. Solids* 10 (1959) 333-335.
- [22] Georg K.H. Madsen, David J. Singh, BoltzTraP. A code for calculating band-structure dependent quantities, *Computer Physics Communications* 175 (2006) 67-71.
- [23] D.M. Rowe, C.M. Bhandari, Modern Thermoelectrics, Holt Saunders, London, 1983, pp.64.
- [24] Mian Liu, Xiaoying Qin, Changsong Liu, Xiyu Li, Xiuhui Yang, Enhanced thermoelectric performance with participation of F-electrons in b-Zn₄Sb₃, *Journal of Alloys and Compounds* 584 (2014) 244-248.
- [25] R.H. Craven, S.F. Meyer, Specific heat and resistivity near the charge-density-wave phase transitions in 2H-TaSe₂ and 2H-TaS₂, *Phys. Rev. B*, 16 (1977) 4583.

- [26] A.H. Thompson, R.F. Gamble and F.R. Koehler Jr, Effects of intercalation on electron transport in tantalum disulfide, *Phys. Rev. B5* (1972) 2811-2816.
- [27] B. Dreyfus and R. Maynard, Analyse de la conductibilité thermique du graphite. - II. théorie, *J. of Phys.* 28 (1967) 955-966.
- [28] M. Bremholm, Y.S. Hor, R.J. Cava, Pressure stabilized Se-Se dimer formation in PbSe₂, *Solid State Sciences* 13 (2011) 38-41.
- [29] John Bosco Balaguru Rayppan, S. Alfred, Cecil Raj, N. Lawrence, Thermal properties of 1T TaS₂ at the onset of charge density wave states, *Physica B Condense Matter* 405 (2010) 3172-3175.
- [30] R. John Bosco Balaguru, S. Alfred, Cecil Raj, N. Lawrence, Lattice Instability of 2H – TaSe₂, *Int. J. Mod. Phys. B* 16 (2002) 4111.
- [31] Arthur P. Ramirez, Superconductivity in alkali-doped C₆₀, *Physica C* 514 (2015) 166–172.
- [32] R. Friend, A.R. Beal, A.D. Yoffe, Electrical and magnetic properties of some first row transition metal intercalates of niobium disulphide, *Phil. Mag.* 35 (1977) 1269.
- [33] E. Doni and R. Girlanda, *Electronic Structure and Electronic Transitions in Layered Materials*, five ed., Grasso, Dordrecht, 1986.
- [34] O. Seifarth, S. Gliemann, M. Skibowski, L. Kipp, On the charge-density-wave mechanism of layered 2H-TaSe₂: photoemission results, *Journal of Electron Spectroscopy and Related Phenomena* 137-140 (2004) 675-679.
- [35] J.P. Tidman, O. Singh, A.E. Curzon, R.H. Friend, The phase transition in 2H-TaS₂ at 75 K, *Phil. Mag.* 30 (1974) 1191.
- [36] Souheyr Meziane, Houda Feraoun, Tarik Ouahrani, Claude Esling, Effects of Li and Na intercalation on electronic, bonding and thermoelectric transport properties of MX₂ (M = Ta; X = S or Se) dichalcogenides – Ab initio investigation, *Journal of Alloys and Compounds* 581 (2013) 731 740.
- [37] R.M. Fleming, R.V. Colman, Superconductivity in Dilute Alloys of TaS₂ with Fe, *Phys. Rev. Lett.* 34 (1975) 1502-1505.
- [38] X.D. Zhu, Y.P. Sun, X.B. Zhu, X. Luo, B.S. Wang, G. Li, Z.R. Yang, W.H. Song, J.M. Dai, Single crystal growth and characterizations of Cu_{0.03}TaS₂ superconductors, *J. Cryst. Growth* 311 (2008) 218.
- [39] C. Haas, Indirect metal-metal interactions in solids: Relation with polarization and charge density waves, *Journal of Solid State Chemistry* 57 (1985) 82-96.
- [40] Paz Vaqueiro, Gerard G Sobany, Fabien Guinet, Patricia Leyva-Bailen, Synthesis and characterisation of the anion-ordered tellurides MGeTe (M = Co, Rh), *Solid State Sciences* 11 (2009) 1077-1082.
- [41] D.E. Monton, J.D. Axe, F.J. Disalvo, Neutron scattering study of the charge-density wave transitions in 2H-TaSe₂ and 2H-NbSe₂, *Phys. Rev. B* 16 (1977) 801.
- [42] M.D. Nunez Regueiro, J.M. Lopez – Castillo, C. Ayache, Thermal Conductivity of 1T- TaS₂ and 2H-TaSe₂, *Phys. Rev. Lett.* 55 (1985) 1931.
- [43] Richard A. Klemm, Pristine and intercalated transition metal dichalcogenide superconductors, *Physica C* 514 (2015) 86–94.
- [44] D. Gutierrez, O. Pena, P. Duran, C. Moure, Crystal Structure, Electrical Conductivity and Seebeck Coefficient of Y(Mn,Ni)O₃ Solid Solution, *Journal of European Ceramic Society* 22 (2002) 567-572.
- [45] F. Zwick, H. Berger, I. Voboni, G. Margaritondo, L. Forro, C. Beeli, M. Onellion, G. Panaccione, A. Taleb-Ibrahimi, M. Grioni, Spectral Consequences of Broken Phase Coherence in 1T- TaS₂, *Phys. Rev. Lett.* 81 (1998) 1058.